



Article

Geochemical Characteristics and Toxic Elements in Alumina Refining Wastes and Leachates from Management Facilities

Chunwei Sun ¹, Jiannan Chen ^{1,2,*}, Kuo Tian ³, Daoping Peng ¹, Xin Liao ^{1,*} and Xiyong Wu ¹

¹ Faculty of Geosciences and Environmental Engineering, Southwest Jiaotong University, Chengdu 611756, Sichuan Province, China; sunchunwei0310@gmail.com (C.S.); pdp0330@swjtu.cn (D.P.); wuxiyong@swjtu.edu.cn (X.W.)

² State-Province Joint Engineering Research Lab in Spatial Information Technology for High Speed Railway Operation Safety, Southwest Jiaotong University, Chengdu 611756, Sichuan Province, China

³ Department of Civil, Environmental, and Infrastructure Engineering, George Mason University, Fairfax, VA 22030, USA; ktian@gmu.edu

* Correspondence: jchen@swjtu.edu.cn (J.C.); xinliao@swjtu.edu.cn (X.L.); Tel.: +86-184-820-391-99 (J.C.); Tel.: +86-138-800-744-12 (X.L.)

Received: 27 February 2019; Accepted: 4 April 2019; Published: 11 April 2019



Abstract: A nationwide investigation was carried out to evaluate the geochemical characteristics and environmental impacts of red mud and leachates from the major alumina plants in China. The chemical and mineralogical compositions of red mud were investigated, and major, minor, and trace elements in the leachates were analyzed. The mineral and chemical compositions of red mud vary over refining processes (i.e., Bayer, sintering, and combined methods) and parental bauxites. The main minerals in the red mud are quartz, calcite, dolomite, hematite, hibschite, sodalite, anhydrite, cancrinite, and gibbsite. The major chemical compositions of red mud are Al, Fe, Si, Ca, Ti, and hydroxides. The associated red mud leachate is hyperalkaline (pH > 12), which can be toxic to aquatic life. The concentrations of Al, Cl⁻, F⁻, Na, NO₃²⁻, and SO₄²⁻ in the leachate exceed the recommended groundwater quality standard of China by up to 6637 times. These ions are likely to increase the salinization of the soil and groundwater. The minor elements in red mud leachate include As, B, Ba, Cr, Cu, Fe, Ni, Mn, Mo, Ti, V, and Zn, and the trace elements in red mud leachate include Ag, Be, Cd, Co, Hg, Li, Pb, Sb, Se, Sr, and Tl. Some of these elements have the concentration up to 272 times higher than those of the groundwater quality standard and are toxic to the environment and human health. Therefore, scientific guidance is needed for red mud management, especially for the design of the containment system of the facilities.

Keywords: red mud; alumina refining; leachate; geochemical characteristics; toxic elements; pH

1. Introduction

Red mud is an insoluble residue produced by aluminum oxide (alumina) refining process with the characteristics of very fine particle size and high alkalinity [1]. In 2015, 274 million tons of bauxite ore were mined globally for alumina production, with Australia (33%), China (20%) and Brazil (16%) being the leading bauxite producers in the world [2]. Approximately 60 million tons of red mud is produced each year globally, with 6 million tons of red mud occurring in China. However, approximately 85% of the red mud is stored in the on-site reservoirs near the alumina refining plant. The reservoir is constructed with dams for containment purposes, and the red mud is treated by a natural settlement process [3].

Currently, manufacturers often adopt the chemical ore dressing process for alumina refining. This process uses the alkali method (sodium hydroxide or sodium carbonates) to produce alumina

from bauxite and can be divided into the Bayer process, the sintering method, and the combined method [4,5]. The main components of the red mud are hematite (Fe_2O_3), calcite (CaCO_3), cancrinite ($\text{Na}_6\text{CaAl}_6\text{Si}_6(\text{CO}_3)\text{O}_{24}\cdot 2\text{H}_2\text{O}$), hydrogarnet ($\text{Ca}_3\text{AlFe}(\text{SiO}_4)(\text{OH})_8$), tricalcium aluminate ($\text{Ca}_3\text{Al}_2(\text{OH})_{12}$), and sodalite ($(\text{Na}_6\text{Al}_6\text{Si}_6\text{O}_{24})\cdot(2\text{NaX or Na}_2\text{X})$) [4,6]. Red mud has strong alkalinity and salinity, with heavy metal elements, including arsenic (As), lead (Pb), zinc (Zn), copper (Cu), nickel (Ni), chromium (Cr), and vanadium (V). The salinity and alkalinity of red mud can affect plant growth and lead to deterioration of soil quality. The leakage or spill of red mud releases oxyanionic trace elements such as Cr, molybdenum (Mo), and V. These contaminants have been reported to be highly soluble under high pH conditions (material pH of red mud) in leaching tests [6,7], suggesting that red mud could be a potential sink of contaminants [8].

Red mud typically occupies land spaces for storage and further generates potential threats to the surrounding environment. Unlined or inappropriately lined red mud reservoirs could induce the leakage of leachate (i.e., bauxite liquor), leading soil swampiness and groundwater pollution [9,10]. Additionally, occasional dam failures damage infrastructure and contaminate the environment. For example, the catastrophic dam failure of the Ajkai Timfoldgyar Zrt red mud reservoir that occurred in Hungary released of 0.7 to 1 million m^3 of caustic red mud into the Torna River, which resulted in the loss of lives and seriously contaminated soil and water [6,9–11].

Overall, the environmental risks are closely related to the soda content, alkalinity, and heavy metal content in the red mud. However, there is still a lack of knowledge regarding the mineralogy and chemical composition within red mud and its leachates in China. The objective of this study is to understand the potential contamination by red mud and its associated leachates from red mud management facilities. The chemical compositions of red mud from different resources and production process are summarized. As red mud leachate has essential effects on the environment, the leaching ability of red mud and its environmental impacts were studied through the analysis of the concentration of elements in leachates. Fresh red mud and its leachates were sampled from the major alumina manufacturers in China. The main chemical parameters, including pH, electrical conductivity (EC), redox potential (ORP), and elemental concentration, were evaluated through laboratory analytical methods.

2. Materials and Methods

2.1. Resources and Distribution of Bauxite

Bauxite is the primary aluminum ore composed of one or more aluminum hydroxides minerals, including gibbsite ($\text{Al}(\text{OH})_3$), boehmite ($\gamma\text{-AlO}(\text{OH})$), diaspore ($\alpha\text{-AlO}(\text{OH})$), and impurities such as quartz (SiO_2), hematite ($\alpha\text{-Fe}_2\text{O}_3$), and rutile (TiO_2) [4,12,13]. Bauxite resources in China are primarily distributed among seven provinces: Shanxi, Henan, Guangxi, Guizhou, Yunnan, Chongqing, and Shandong. Diaspore is the primary type of bauxite in China and contains 37.4~74.0% of Al_2O_3 and 3.5~32.2% of SiO_2 [4,14–18]. The average Al_2O_3 content of bauxites in Guangxi varies between 52.3% and 62.4%, and the average Fe_2O_3 and SiO_2 contents range between 15.0~24.5% and 3.5~8.3% (Table 1). However, the SiO_2 contents (7.5~32.2%) in bauxite from Henan, Shandong, Shanxi, and Guizhou are higher than those from Guangxi, which result in a lower Al/Si ratio (1.2~9.4) than that of Guangxi bauxite (6.3~17.8).

The Al/Si ratio determines the alumina processing procedure. In general, Guangxi aluminum mines are bauxite deposits with a high Al/Si ratio (6.3–17.8). This type of bauxite can be utilized to extract alumina using the Bayer process. Shanxi, Shandong, Henan, Guizhou, and Sichuan aluminum mines, which account for over 98% of the reserves in China, are mainly bauxite deposits with a relatively low Al/Si ratio (3.3–9.4). These types of ores are middle/low-grade diaspore bauxites. They are usually challenging and energy consuming to process for alumina. Therefore, alternative methods modified from the traditional Bayer process, i.e., the sintering process and the Bayer-sintering combined process, have been developed for alumina refining [4].

Table 1. The major chemical compositions (oxide wt.%), loss on ignition (LOI, wt.%) and Al/Si in bauxite over the world.

Bauxite Origin	Al ₂ O ₃	Fe ₂ O ₃	SiO ₂	TiO ₂	MgO	K ₂ O	CaO	Na ₂ O	LOI	Al/Si	Ref.
Juruti, Brazil	45.0	14.7	24.9	1.9	-	-	-	-	18.2	1.8	[19]
Mandan, Iran	44.4–64.1	2.8–22.3	3.3–9.6	2.1–3.2	0.1–0.3	0.02–0.3	0.05–11.3	0.02–0.07	11.1–23.2	5.4–15.8	[20]
Kanisheeteh, Iran	20.2–33.4	17.2–34.2	23.6–43.6	3.1–4.8	0.01–0.7	0.02–1.3	0.1–0.4	0.01–0.9	6.0–9.7	0.5–1.4	[21]
Rompin, Malaysia	29.0–44.4	2.5–4.0	28.8–52.5	0.2–0.3	>0.01	0.05–0.1	-	-	13.9–24.1	0.55–1.54	[22]
Kuantan, Malaysia	41.3–43.6	20.7–23.5	3.1–11.9	3.5–4.1	0.08–0.09	-	-	-	22.0–25.2	3.5–14.0	[22]
Johor, Malaysia	43.4–50.6	15.1–17.3	3.7–13.8	2.4–2.3	-	-	-	-	22.8–28.0	3.1–13.7	[22]
Guangxi, China	52.3–62.4	16.6–24.5	3.5–8.3	1.9–3.2	0.02–0.09	0.004–0.03	0.03–0.1	0.001–0.2	11.8–17.7	6.3–17.7	[14]
Henan, China	63.3–69.4	1.5–9.4	8.7–18.0	0.7–3.2	-	-	-	-	12.8–14.7	3.4–7.6	[15]
Shandong, China	37.4	8.7	32.2	2.3	0.9	-	3.2	0.9	13.7	1.2	[16]
Guangxi, China	58.6	15.0–17.0	5.0–6.0	-	-	-	-	-	-	9.9	[17]
Guizhou, China	67.0–68.0	2.2–3.0	8.8–11.1	-	-	-	-	-	-	6.1–7.8	[17]
Henan, China	64.0–74.0	3.0–5.1	7.5–13.7	-	-	-	-	-	-	4.7–9.4	[17]
Shandong, China	54.0–61.0	5.0–9.0	15.0–22.0	-	-	-	-	-	-	3.7–3.9	[17]
Shanxi, China	63.0–65.0	2.0–3.0	11.0–13.0	-	-	-	-	-	-	5.0–5.6	[17]
Henan, China	66.8	1.4	12.5	3.0	0.1	0.3	0.3	0.04	14.2	5.4	[18]
France	58.6	26.2	0.8	2.8	-	-	-	-	-	73.3	[23]
France	76.4	4.8	0.8	3.3	-	-	-	-	-	95.5	[23]
France	60.6	26	0.3	0.8	-	-	-	-	-	209.0	[23]
France	63.7	5.5	13.3	2.4	-	-	-	-	-	4.8	[23]
Romania	59.7	23.7	1.5	3.1	-	-	-	-	-	2.5	[23]
Romania	65.5	21.3	0.8	2.8	-	-	-	-	-	82	[23]
Italy	57.6	26.6	2.8	1.3	-	-	-	-	-	20.7	[23]
Italy	58.9	18.6	7.9	-	-	-	-	-	-	7.4	[23]
Alabama, USA	58.2	3.6	2.9	3.4	-	-	-	-	-	20.1	[23]
Arkansas, USA	62.3	1.7	2.0	3.5	-	-	-	-	-	31.1	[23]
Arkansas, USA	55.1	6.1	10.1	-	-	-	-	-	-	5.4	[23]
Georgia, USA	64.9	0.3	0.6	1.1	-	-	-	-	-	104.7	[23]
Guyana, UK	64.4	0.5	2.7	0.1	-	-	-	-	-	23.6	[23]
Guyana, UK	70.9	0.8	1	1.1	-	-	-	-	-	70.9	[23]

2.2. The Sampling of Red Mud and Leachate

In this study, samples of red mud and leachates from five management facilities were collected from three provinces (i.e., Guangxi, Shangdong, and Henan) in China (Figure 1). The details of the sampling are summarized in Table 2. Fresh red mud samples GX-A1 and GX-A2, and leachate samples GX-A2-L and GX-A2-L were collected from the same manufacturer but two adjacent reservoirs (A1 and A2, respectively) in Pingguo County, Guangxi Province. The average annual temperature of Pingguo County is 21.5 °C, and the annual precipitation reaches 1500 mm. Fresh red mud sample GX-B and leachate sample GX-B-L were collected in Jingxi County, Guangxi Province. The average annual temperature of Jingxi County is 19.1 °C, and the annual precipitation reaches 1636 mm. Red mud sample SD-A and its leachate sample SD-A-L were collected in Zibo, Shandong. The average annual temperature of Zibo is 13.5 °C, and the annual precipitation reaches 650 mm. Red mud sample HN-A and its leachate sample HN-A-L were collected in Xingyang, Henan Province. The average annual temperature is 14.3 °C, and the annual precipitation reaches 645 mm. Fresh red mud was sampled after pressure filtration, and the leachate was collected from the drainage pipe of the red mud reservoir.

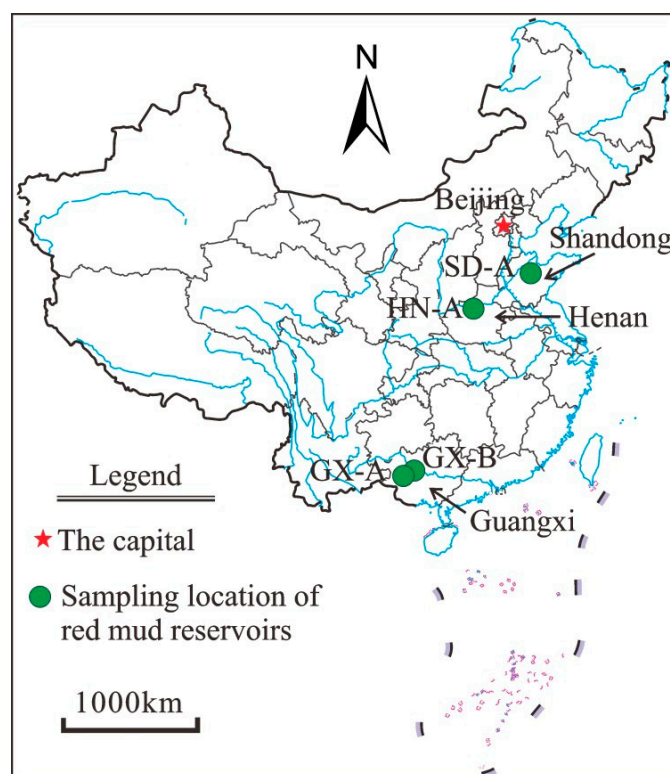


Figure 1. Locations for red mud and leachate sampling of the current study.

Table 2. Sampling program of red mud and its associated leachate from the red mud reservoirs in China.

Locations	Red Mud Reservoirs	Types of Samples	Processes Method
Guangxi	3 Reservoirs (denoted as GX-A1, GX-A2, and GX-B)	Bauxite residual,	Combined and Bayer
Shandong	1 Reservoirs (denoted as SD-A)	Leachate	Bayer
Henan	1 Reservoir (denoted as HN-A)		Sintering

2.3. Bulk Chemical Analysis

Specimens were analyzed using X-ray fluorescence (XRF) quantitative analysis (Shimadzu XRF-1800, Kyoto, Japan). The analytical method for silicate rocks was used, and specimens were analyzed in duplicates. Five grams of each sample was air-dried for 24 h and ground to <0.075 mm

with agate mortar and pestle. Loss on ignition tests were performed before XRF analysis by sintering samples at 900 °C using a muffle furnace (YSD-5-12T, Yaoshi Instrument Equipment Ltd., Shanghai, China). The LOI is used as an indicator for organic contents in the samples. XRF tests were conducted by fusing 0.9 g of calcined powder (i.e., specimen after LOI) with 1 g of NH_4NO_3 oxidizer and 9.0 g of lithium borate flux (50%/50% $\text{Li}_2\text{B}_4\text{O}_7$ - LiBO_2) at 1050 °C into a flat molten glass disk. The specimens were then analyzed by XRF spectrometry.

2.4. Mineralogical Analysis

Quantitative X-ray diffraction analysis (Rigaku D/MAX-2005 X-ray diffractometer, Tokyo, Japan) was performed on the red mud samples to determine the major mineral phases. Specimens were placed in a desiccator for 24 h and ground to 0.075 mm with agate mortar and pestle. $\text{Cu K}\alpha$ radiation was used, and each sample was placed in a 2-mm deep sample holder and scanned at 0.02° intervals between 5° to 50° 2 θ with a 2 s dwell time. Samples were scanned within 48 h after desiccation to minimize crystal dehydration.

2.5. Hydrochemical Analysis

pH, EC, and ORP of leachate samples were recorded immediately after sampling. Leachate samples were then filtered through a 0.45- μm filter paper and preserved with trace-grade nitric acid (HNO_3). The elemental concentrations of silver (Ag), aluminum (Al), As, beryllium (Be), boron (B), barium (Ba), calcium (Ca), cadmium (Cd), cobalt (Co), Cr, Cu, iron (Fe), mercury (Hg), potassium (K), lithium (Li), magnesium (Mg), manganese (Mn), Mo, sodium (Na), Ni, Pb, antimony (Sb), selenium (Se), silicon (Si), strontium (Sr), titanium (Ti), thallium (Tl), V, and Zn were determined by Inductively Coupled Plasma Mass Spectrometry (ICP-MS, Agilent Technologies 700 Series, Santa Clara, CA, USA) at Chengdu University of Science and Technology. Anions, including chloride (Cl^-), fluoride (F^-), nitrate (NO_3^-), and sulfate (SO_4^{2-}), were determined by ion chromatography (IC, Shimadzu HIC-SP, Kyoto, Japan) at Southwest Jiaotong University.

3. Results

3.1. Chemical and Mineral Compositions of Red Mud

The chemical and mineralogical compositions of red mud in China from this study and the literature are summarized in Tables 3 and 4, respectively. The major chemical components of red mud are SiO_2 , TiO_2 , Al_2O_3 , Fe_2O_3 , CaO, and Na_2O . These components comprise 69.5–98.3% of the total mass of the red mud. Na mainly comes from the sodium hydroxide (NaOH), which is used to treat bauxite, while Al, Si, Fe, Ti, and other elements are derived from the parental bauxite. The secondary components are K_2O , MgO, P_2O_5 , MnO, Cr_2O_3 , and SO_3 . The main mineral phases include quartz (SiO_2), calcite (CaCO_3), dolomite ($\text{CaMg}(\text{CO}_3)_2$), hematite (Fe_2O_3), hydrogarnet ($\text{Ca}_3\text{Al}_2(\text{SiO}_4)_2(\text{OH})_4$), sodalite ($\text{Na}_8(\text{Al}_6\text{Si}_6\text{O}_{24})\text{Cl}_2$), anhydrite (CaSO_4), cancrinite ($\text{Na}_6\text{Ca}_2((\text{CO}_3)_2\text{Al}_6\text{Si}_6\text{O}_{24})\cdot 2\text{H}_2\text{O}$), and gibbsite ($\text{Al}(\text{OH})_3$).

The SiO_2 content of red mud ranges from 8.4% to 32.5%. SiO_2 is leached from kaolinite ($\text{Al}_2\text{Si}_2\text{O}_3(\text{OH})_4$) in bauxite during alumina refining and exists in the form of hydrophane ($\text{SiO}_2\cdot n\text{H}_2\text{O}$) and sodium silicate (Na_2SiO_3) [24]. In general, the red mud samples derived from Guangxi and Yunnan have lower SiO_2 contents (8.4–11.9%) than those from Henan, Shandong, Shanxi and Guizhou (up to 32.5%) (Figure 2 and Table 3). This difference is mainly due to the different Si-Al ratio of bauxite ores. The Fe_2O_3 content of red mud ranges from 2.5% to 37.0% (Table 3). Fe is mainly in the form of $\text{Fe}(\text{OH})_3$, which is the oxidation and hydration product of FeS_2 in bauxite. $\text{Fe}(\text{OH})_3$ is unstable under strong alkaline and high-temperature conditions, and easily converts into goethite (FeOOH). In fresh red mud, $\text{Fe}(\text{OH})_3$ and FeOOH may coexist, and FeO may exist in the form of siderite (FeCO_3). The Al_2O_3 content of red mud ranges from 6.4 to 31.0% (Table 3), and Al_2O_3 usually exists in two forms, i.e., NaAlO_2 and $\text{Al}(\text{OH})_3$, under strongly alkaline conditions. The CaO content ranges from

2.2% to 48.4% (Table 3), and CaO usually forms aragonite (CaCO_3) or calcite (CaCO_3). CaCO_3 can deposit and crystallize after the introduction of quicklime (CaO) and carbon dioxide (CO_2) during alumina production. The content of Na_2O in red mud ranges from 2.3% to 16.2% (Table 3) and exists in pore solutions as free Na^+ . In addition, a series of saline deposits or colloid products, such as Na_2CO_3 , NaHCO_3 , Na_2SiO_3 , and NaAlO_2 , are formed during desiccation. The Ti_2O content ranges from 0.05% to 7.0% (Table 3). Ti_2O exists as rutile and anatase in bauxite.

Table 3. The major chemical compositions (Oxide wt.%) of red mud in China.

Refinery	Process	SiO_2	Al_2O_3	Fe_2O_3	CaO	TiO_2	Na_2O	MgO	K_2O	Cr_2O_3	P_2O_5	SO_3	MnO	LOI	Refs.	
HN-A	Bayer	22.5	25.3	8.1	15.1	3.8	8.8	1.3	1.2	0.1	0.3	-	0.1	12.1	This Study	
SD-A	Bayer	16.7	20.4	23.7	13.6	4.9	8.0	0.4	0.2	0.1	0.3	0.4	-	11.2		
GX-A1	Bayer	16.6	23.8	30.6	2.2	6.9	9.7	0.2	0.1	0.1	0.3	0.4	-	9.1		
GX-B	Bayer	15.3	20.5	21.2	14.5	5.7	8.1	0.7	0.1	0.3	0.2	0.7	0.1	12.5		
GX-A2	Bayer	16.4	19.1	22.0	16.0	5.0	7.6	0.9	0.1	0.2	0.2	0.3	0.1	12.0		
Guangxi	Bayer	9.1	18.7	37.0	6.0	6.4	3.4	-	-	-	-	-	-	-		[25]
Guangxi	Bayer	8.4	18.5	31.3	18.1	6.2	3.2	0.7	0.2	0.3	-	0.3	0.7	13.9		[26]
Guangxi	Bayer	11.9	17.5	32.5	14.1	5.5	4.0	-	1.0	-	-	-	-	-		[27]
Guangxi	Bayer	11.9	19.5	29.9	13.9	3.4	4.6	2.8	-	-	-	-	-	11.6		[28]
Guangxi	Bayer	8.9	18.9	34.3	13.6	6.1	4.4	0.4	0.1	-	-	-	-	-		[5]
Henan	Bayer	20.6	25.5	11.8	14.0	4.1	6.6	1.5	2.1	-	-	-	-	-	[5]	
Henan	Combined	20.4	7.6	8.2	44.7	7.3	3.0	-	-	-	-	-	-	11.0	[29]	
Henan	Sintering	21.4	8.8	8.6	36.0	2.6	3.2	1.9	0.8	-	-	-	-	16.3	[30]	
Henan	Bayer	18.6	23.0	12.4	15.7	4.1	4.5	1.6	1.8	-	-	-	-	12.5	[8]	
Henan	Combined	22.5	7.0	8.1	44.1	7.3	2.4	2.0	0.5	-	-	-	-	8.3	[30]	
Henan	Sintering	17.2	8.1	9.8	37.0	4.7	2.5	1.0	2.5	-	0.3	-	0.0	17.0	[31]	
Henan	Sintering	20.9	7.0	7.2	48.4	3.2	2.3	-	-	-	-	-	-	-	[32]	
Shandong	Sintering	32.5	8.3	5.7	41.6	-	2.3	-	-	-	-	-	-	-	[5]	
Shandong	Sintering	19.1	8.8	12.2	35.5	2.4	3.9	1.9	0.4	-	-	0.3	-	-	[33]	
Shandong	Sintering	19.1	6.9	12.8	46.0	3.4	2.4	1.2	1.2	-	-	-	-	5.7	[34]	
Shandong	Sintering	22.0	6.4	9.0	41.9	3.2	2.8	1.7	0.3	-	-	-	-	11.7	[30]	
Shandong	Sintering	22.7	7.7	11.0	40.8	3.3	2.9	1.8	0.4	-	-	-	-	11.8	[35]	
Yunnan	Bayer	11.2	17.5	35.3	12.4	2.4	8.1	1.6	-	-	-	-	-	10.0	[36]	
Yunnan	Bayer	8.6	18.2	29.4	11.0	0.1	3.2	-	0.1	-	-	9.3	-	-	[29]	
Shanxi	Combined	22.2	10.5	6.8	42.3	2.6	3.0	2.5	0.9	-	-	-	-	-	[5]	
Shanxi	Sintering	18.1	9.2	4.7	38.1	6.7	4.0	-	-	-	-	-	-	12.3	[37]	
Shanxi	Bayer	17.4	23.6	4.2	20.2	6.9	8.6	-	-	-	-	-	-	11.5	[37]	
Shanxi	Bayer	16.7	23.5	9.2	16.1	4.8	6.3	-	-	-	-	-	-	12.2	[37]	
Shanxi	Sintering	16.4	6.8	7.6	33.1	2.5	3.0	1.7	0.2	-	-	-	-	-	[24]	
Shanxi	Combined	21.4	8.2	8.1	46.8	2.9	2.8	1.7	0.2	-	-	-	-	-	[32]	
Shanxi	Bayer	17.8	24.7	10.4	15.7	5.4	9.8	0.9	0.6	-	-	-	-	-	[32]	
Guizhou	Bayer	16.7	33.2	8.2	19.6	4.3	16.2	0.7	0.6	-	-	-	-	1.7	[34]	
Guizhou8	Bayer	14.3	20.0	16.0	20.0	5.5	9.2	0.9	2.0	-	-	-	-	12.3	[34]	
Guizhou	Bayer	15.7	27.3	7.7	21.5	4.8	15.4	1.7	2.8	-	-	-	-	3.8	[34]	
Guizhou	Sintering	20.4	10.8	9.1	34.3	4.1	5.3	1.2	5.3	-	-	-	-	14.1	[34]	
Guizhou	Bayer	12.4	31.0	2.5	23.7	5.7	4.3	0.7	0.5	-	-	-	-	16.5	[31]	
Guizhou	Sintering	21.0	8.1	6.2	45.1	5.2	2.8	-	0.1	-	-	-	-	9.4	[31]	

Table 4. The mineral compositions (wt.%) of red mud sampled in this study.

Mineral	Formula	HN-A	SD-A	GX-A	GX-B	SD-B
Quartz	SiO_2	10	10	-	-	10
Calcite	CaCO_3	-	20	10	10	-
Dolomite	$\text{CaMg}(\text{CO}_3)_2$	-	-	-	-	-
Hematite	Fe_2O_3	20	40	35	35	50
Hydrogarnet	$\text{Ca}_3\text{Al}_2(\text{SiO}_4)_2(\text{OH})_4$	40	-	30	30	-
Sodalite	$\text{Na}_8(\text{Al}_6\text{Si}_6\text{O}_{24})\text{Cl}_2$	30	20	-	25	-
Anhydrite	CaSO_4	-	10	-	-	-
Cancrinite	$\text{Na}_6\text{Ca}_2((\text{CO}_3)_2\text{Al}_6\text{Si}_6\text{O}_{24})\cdot 2\text{H}_2\text{O}$	-	-	25	-	-
Gibbsite	$\text{Al}(\text{OH})_3$	-	-	-	-	40

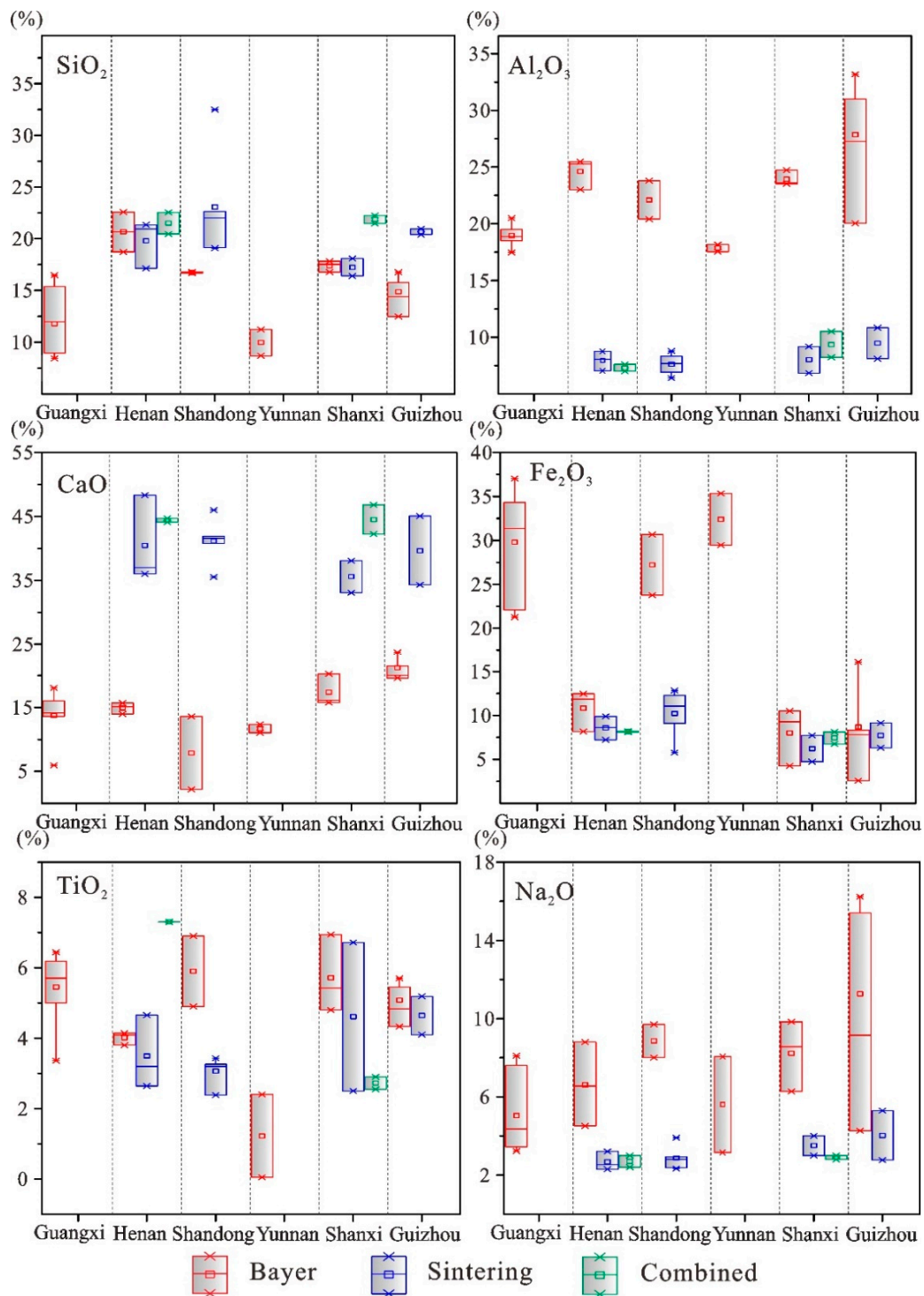


Figure 2. Box plot of chemical composition in Red Mud from the alumina manufactures in China.

3.2. The Hydrochemistry of Red Mud Leachate and Its Major Elements

Hydrochemical parameters of the red mud leachate samples include pH, EC, ORP, and ionic strength are summarized in Table 5. The pH of red mud leachate ranges from 12.1 to 12.6, which exceeds the Integrated Wastewater Discharge Standard in China (IWDS) (GB8978-1996). The ionic strength ranges from 66.9 to 484.3 mM, and the EC value of red mud leachate ranges from 4.4 to 51.1 mS/cm which exceeds the standard (EC value less than 2.0 mS/cm) for reverse osmosis water

treatment system. The ORP ranges from −110.0 to −29.0 mV, indicating a reducing state of the red mud leachate.

Table 5. Bulk chemical parameters of red mud leachate samples from the current study.

Leachate Samples	Sample Location	pH	EC@25 °C (mS/cm)	ORP (mV)	Ionic Strength (mM) *
HN-A-L	Leachate drainage	12.6	27.6	−72.0	383.3
SD-A-L		12.6	51.1	−110.0	484.3
GX-A1-L		12.6	4.4	−29.0	66.9
GX-B-L		12.4	26.3	−63.0	238.8
GX-A2-L		12.1	9.71	−46.0	159.5

* Calculated using Visual MINTEQ, charge differences <5%.

Al, Ca, Na, K, Mg, Si, Cl[−], F[−], NO₃^{2−}, and SO₄^{2−} are the major elements and ions (defined based on the concentrations) in the red mud leachate (Figure 3 and Table 6). The maximum contamination levels (MCLs) of type (III) (for drinking water) groundwater of the Quality Standard for Groundwater in China (China (GW)) (GB/T 14848-2017) and US Environment Protection Agency Groundwater Quality Standard (USEPA (GW)) were used to evaluate the possible harmfulness of leachate to the environment and human health.

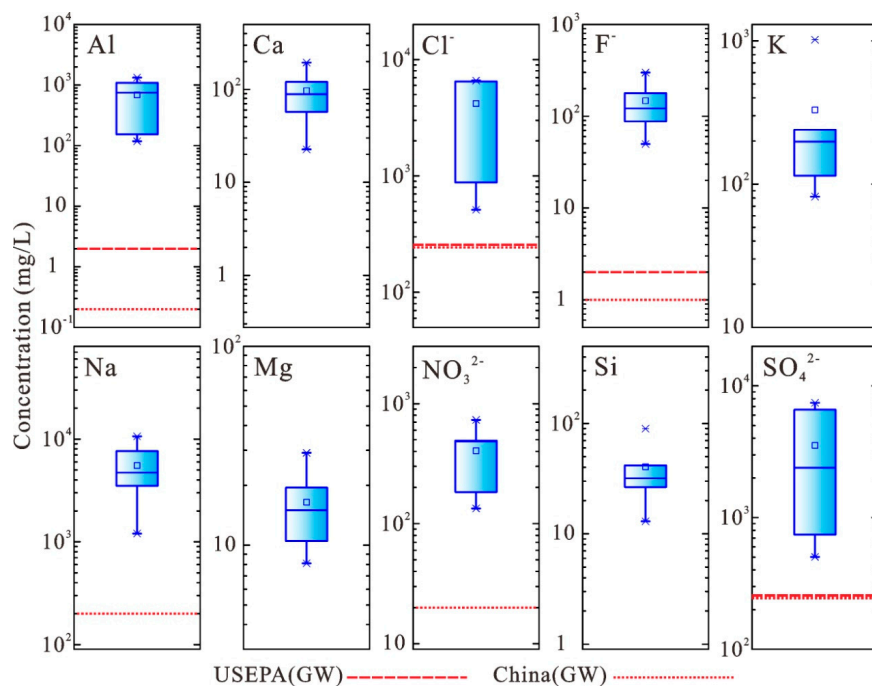


Figure 3. Boxplot of the concentration of major elements/ions in red mud leachate (Red lines indicates the MCLs of groundwater quality standards).

Table 6. The concentration of major elements (ions) in the red mud leachate (mg/L).

Samples	Al	Ca	Na	Mg	K	Si	Cl [−]	F [−]	NO ₃ [−]	SO ₄ ^{2−}
HN-A-L	1327.4	22.6	7634.5	8.1	1016.0	31.8	6588.1	299.6	492.2	2386.4
SD-A-L	745.5	57.1	10650.0	10.5	81.8	89.9	6490.5	121.8	483.4	7453.3
GX-A1-L	118.3	120.6	1200.5	19.5	114.4	13.0	511.4	88.0	183.2	502.5
GX-B-L	152.9	194.6	4707.0	29.1	197.6	26.5	6459.8	178.6	730.7	6593.0
GX-A2-L	1095.5	88.9	3506.0	15.0	239.3	41.7	877.1	49.8	133.8	741.7
Range	118.3–1327.4	22.6–194.6	1200.5–10650.0	8.1–29.1	81.8–1016.0	13.8–89.9	511.4–6588.1	88.0–299.6	183.2–730.7	502.5–6593.0
USEPA (GW)	2	-	-	-	-	-	250	2	-	250
China (GW)	0.2	-	200	-	-	-	250	1	20	250

The Al concentration in red mud leachate ranges from 118.3 to 1327.4 mg/L, which exceeds the recommended values set by USEPA (GW) (2 mg/L) and China (GW) (0.2 mg/L). Na concentrations in the red mud leachate range from 1200.5 to 10,650.0 mg/L, which is 6002.5 to 53,250 times higher than the recommended value by China (GW) (0.2 mg/L). Additionally, Cl⁻, as one of the main anions found in the leachate solution of red mud, has a concentration ranging from 551.4 to 6588.1 mg/L. This range is 2.2 to 26.4 times higher than the recommended value of USEPA (GW) and China (GW) (250 mg/L). The F⁻ concentration in the leachate ranges from 88.0–299.6 mg/L, which is more than 44 times higher than the recommended value of USEPA (GW) (2 mg/L) and China (GW) (1 mg/L). The concentration of NO₃²⁻ ranges from 183.2–730.7 mg/L, which is 9.2 to 36.5 times higher than the recommended value of China (GW) (20 mg/L). The concentration of SO₄²⁻ ranges from 502.5–6593.0 mg/L, which is 2.0 to 26.4 times higher than the recommended value of USEPA (GW) and China (GW) (250 mg/L). Pyrite (FeS₂) in bauxite is likely the primary source of SO₄²⁻ [38].

3.3. The Minor and Trace Elements in Red Mud Leachate

The minor elements of the red mud leachates mainly include As, B, Ba, Cr, Cu, Fe, Ni, Mn, Mo, Ti, V, and Zn (Figure 4 and Table 7). Elements, such as, Cr, and V, form oxyanions under alkaline conditions (pH >10) and are highly soluble in the water [39]. The concentration ranges of these elements are: 0.2–2.0 mg/L for As, 9.7–163.4 mg/L for B, 0.1–0.5 mg/L for Ba, 0.1–5.9 mg/L for Cr, 0.2–1.6 mg/L for Cu, 0.7–15.0 mg/L for Fe, 0.8–1.0 mg/L for Ni, 0.3–0.6 mg/L for Mn, 1.0–14.5 mg/L for Mo, 0.2–1.8 mg/L for Ti, 0.9–6.3 mg/L for V, and 4.2–37.0 mg/L for Zn. The MCLs of type (III) (for drinking water) groundwater of the Quality Standard for Groundwater in China (China (GW)) (GB/T 14848–2017), US Environment Protection Agency Groundwater Quality Standard (USEPA (GW)), and Integrated Wastewater Discharge Standard (IWDS) (GB8978-1996) were used to evaluate the possible harmfulness of leachate to the environment and human health.

Table 7. The concentration of minor elements (ions) in red mud leachate (unit: mg/L).

Samples	As	B	Ba	Cr	Cu	Fe	Ni	Mn	Mo	Ti	V	Zn
HN-A-L	0.2	163.5	-	0.1	0.2	1.5	0.8	0.4	1.0	1.0	2.1	37.0
SD-A-L	1.8	39.7	0.1	5.9	1.6	15.0	0.9	0.3	14.5	1.8	6.3	18.3
GX-A1-L	2.0	9.7	0.3	0.9	0.4	2.4	1.1	0.6	2.8	0.6	6.3	4.2
GX-B-L	0.8	10.1	0.5	0.1	0.2	0.9	1.0	0.4	4.2	1.1	0.9	1.1
GX-A2-L	0.8	13.8	0.1	0.1	0.4	0.7	1.0	0.3	2.0	0.2	1.5	13.9
Range	0.2–2.0	9.7–163.4	0.1–0.5	0.1–5.9	0.2–1.6	0.7–15.0	0.8–1.0	0.3–0.6	1.0–14.5	0.2–1.8	0.9–6.3	4.2–37.0
USEPA (GW)	0.01	-	2	0.1	1.3	0.3	-	0.05	-	-	-	-
China (GW)	0.01	0.5	0.7	0.05*	1	0.3	0.02	0.1	0.07	-	-	1
IWDS	0.5	-	-	1.5	2.0	-	1.0	2.0	-	-	2.0	5.0

* MCL of Cr(VI).

Exceedance was found for most of the minor elements. The concentration of As is 20 to 200 times higher than the MCL of USEPA (GW), China (GW). The concentration of B is 19.4 to 326.8 times higher than the MCL of China (GW) (0.5 mg/L). The Cr concentration is 2 to 118 times higher than the MCL of China (GW) (0.05 mg/L). The Fe concentration is 2.3 to 50 times higher than the MCL of China (GW) and USEPA (GW) (0.3 mg/L). The Ni concentration is 40 to 50 times higher than the MCL of China (GW) (0.02 mg/L). The Mn concentration is 6 to 12 times higher than the MCL of USEPA (GW) (0.05 mg/L). The Mo concentration is 14.3 to 207 times higher than the MCL of China (GW) (0.07 mg/L). The Zn concentration is 4.2 to 37.0 times higher than the MCL of China (GW) (1 mg/L).

Trace elements of the red mud leachate mainly include Ag, Be, Cd, Co, Hg, Li, Pb, Sb, Se, Sr, and Tl (Figure 5 and Table 8). The concentrations of these elements are: 2.0–197.0 µg/L for Ag, 52.0 µg/L for Be (only detected in GX-A2-L), 12.0–172.0 µg/L for Cd, 22.0–88.0 µg/L for Co, 275.0–599.0 µg/L for Hg, 28.0–893.0 µg/L for Li, 170.0–1096.0 µg/L for Pb, 14.0–71.0 µg/L for Sb, 525.0–1359.0 µg/L for Se, 100.0–750.0 µg/L for Sr, and 5.0 µg/L for Tl (only detected in GX-A1-L). Meanwhile, the concentrations of elements Ag, Be, Cd, Co, Hg, Pb, Sb, Se, and Tl are 2.4 to 272.0 times higher than the MCLs of the

China (GW) or USEPA (GW). However, the MCLs of IWDS are much higher than those for drinking ground-water. The concentrations of the minor and trace elements, such as As, Cr, Ni, Mn, Zn, Be, Cd, Pb, Hg, and Se exceed the MCLs of IWDS; this indicates that red mud leachate is harmful to the environment and cannot be directly discharged into the river network.

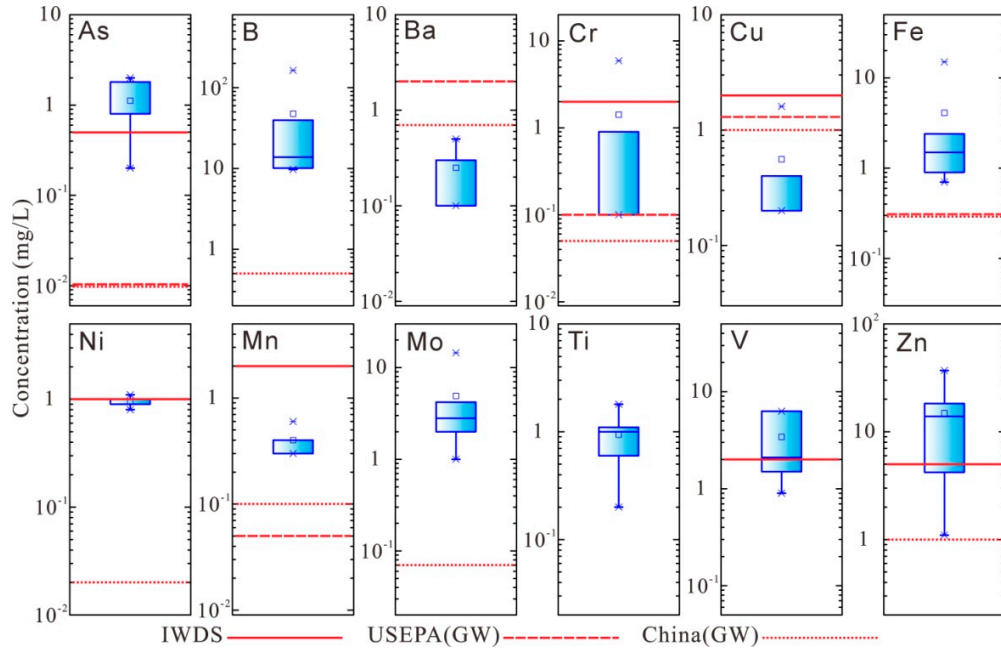


Figure 4. Boxplot of the concentration of minor elements in red mud leachate (Red lines indicates the MCLs of groundwater quality standards).

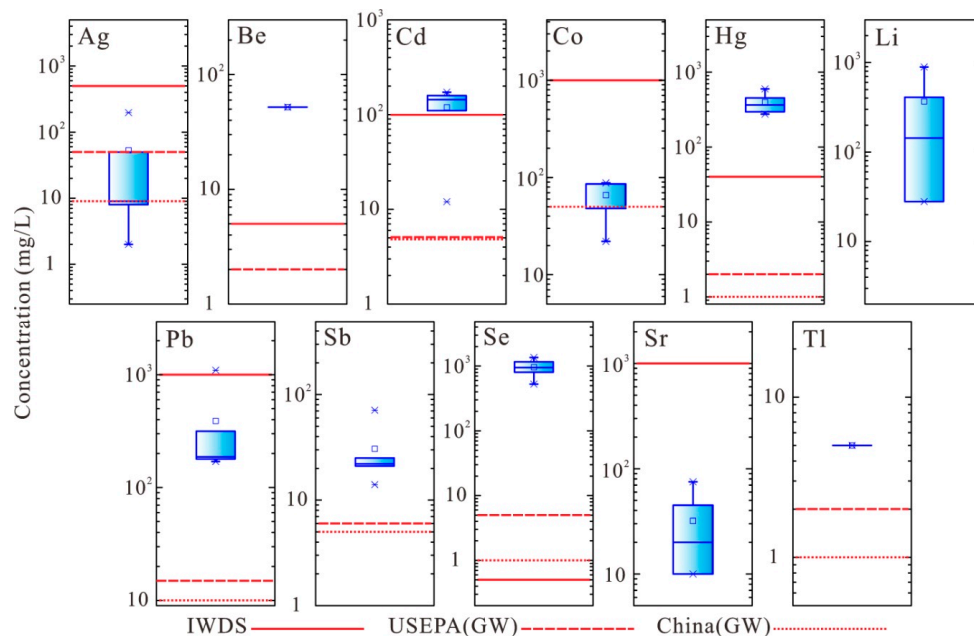


Figure 5. Boxplot of the concentration of trace elements in red mud leachate (Red lines indicates the MCLs of groundwater quality standards).

Table 8. The concentration of trace elements in red mud leachate (unit: µg/L).

Samples	Ag	Be	Cd	Co	Hg(total)	Li	Pb	Sb	Se	Sr	Tl
HN-A-L	9	/	12	22	599	893	187	14	951	100	/
SD-A-L	50	/	144	48	453	409	1095	71	1160	100	/
GX-A1-L	8	/	172	86	296	/	179	22	801	450	5
GX-B-L	2	/	159	86	275	28	170	21	1359	750	/
GX-A2-L	197	52	110	88	365	143	316	25	525	200	/
Range	2–197	≤52	12–172	22.88	275–599	≤893	170–1095	14–71	525–1359	100–750	≤5
USEPA (GW)	50	2	5	-	2	-	15	6	5	-	2
China (GW)	50	2	5	50	1	-	10	5	10	-	0.1
IWDS	500	5	100	1000	50	-	1000	-	0.5	10,000	-

4. Discussion

The bauxite source and extraction processes have a strong impact on the chemical and mineralogical composition of the red mud. For example, the variation in Na₂O contents is partially due to the addition of NaOH. In the Bayer process, NaOH is used to dissolve the Al from Fe-rich aluminite bauxite [40]. However, the sintering and Bayer-sintering combined methods are often adopted to refine alumina from insoluble diaspore or kaolinite type bauxite ores (usually, Al and Si-rich, but low in iron content). Additionally, to enhance the dissolution of alumina and reduce the consumption of alkali, lime is usually added in the high-temperature sintering process. CaCO₃ can deposit and crystallize by introducing lime (CaO) and carbon dioxide (CO₂) during alumina production. Therefore, the associated red mud from sintering or Bayer-sintering combined methods is usually Ca-rich but low in iron content.

Additionally, the content of iron oxide (Fe₂O₃) in the red mud produced by the Bayer process is higher than that in the red mud produced by the sintering process. In the Bayer process, while extracting alumina from the bauxite using aqueous NaOH, Fe₂O₃ is left in the residue. Therefore, the red mud usually presents relatively high contents of Fe₂O₃ [41]. Red mud from the sintering process usually contains elevated CaO contents, while red mud produced by the Bayer process contains elevated Na₂O and Al₂O₃ contents (Figure 2). This difference is due to the addition of limestone in lieu of NaOH (or Na₂CO₃) in the sintering process. The aluminum recovery from the bauxite ore in the Bayer process is lower than in the sintering alumina process [42]. Therefore, Bayer red mud usually contains more alumina (Al₂O₃) than red mud from the sintering process.

A series of saline deposits or colloid products, such as CaCO₃, Na₂CO₃, NaHCO₃, Na₂SiO₃, and NaAlO₂, are formed during desiccation. However, during the wetting process, these deposits can be easily soluble and cause salinization pollution to the land. The high concentration of alkaline substances (usually pH >12) is the primary reason for the classification of residue as a special industrial material in some countries, such as Australia [43]. The alkaline mineral composition of red mud from refining processes consists of natron-decahydrate (Na₂CO₃·10H₂O), calcite (CaCO₃), hydrogarnet (Ca₃Al₂(SiO₄)₂(OH)₄), sodalite (Na₈(Al₆Si₆O₂₄)Cl₂), cancrinite (Na₆Ca₂((CO₃)₂Al₆Si₆O₂₄)·2H₂O). The following dissolution reactions enable the red mud to become strongly alkaline:



The reactions indicate that NaOH, Na₂CO₃, NaHCO₃, and NaAl(OH)₄ are the major soluble alkalinity compounds in red mud. These compounds are formed mainly due to the addition of NaOH, CO₂, and CaO during the alumina production process [4]. The main anions leading to the alkalinity of red mud in the leachate are: OH⁻, CO₃²⁻, HCO₃⁻, Al(OH)₄⁻, H₂SiO₄²⁻, and H₃SiO₄⁻, most of which are the dissolution products of sodalite (Na₈(Al₆Si₆O₂₄)Cl₂), cancrinite (Na₆Ca₂((CO₃)₂Al₆Si₆O₂₄)·2H₂O), hydrogarnet (Ca₃Al₂(SiO₄)₂(OH)₄), and tricalcium aluminate (Ca₃Al₂O₆). However, the alkaline substances of red mud vary with the refining processes. The Bayer red mud is strongly alkaline [9]. Compared with other processes, more caustic soda is added in the Bayer process, resulting in much higher contents in sodium monoxide (Na₂O) in the red mud, with approximately 9.7% being detected in the red mud sample of SD-A (Table 2).

In general, the major elements (including Al, Ca, K, Na, Mg, Si, Cl⁻, F⁻, NO₃²⁻, and SO₄²⁻) all exceeded the recommended value of groundwater quality standards and could increase the risk of salinization of soil and water [7,9]. Al mainly exists as Al(OH)₄⁻ under high pH (pH > 12) conditions, and the insoluble Al(OH)₃ in red mud can easily be converted into soluble Al(OH)₄⁻. NaOH is added during the refining process, therefore, a high concentration of Na is expected to be retained or dissolved in the leachate. In some cases, KOH is added during the refining process, such as in sample HN-A-L, and a higher content of K (1016.0 mg/L) in the leachate can be found than in leachates of other red muds (Table 6). Na or K is the top components for salinization of soil and water [9].

As one of the main anions found in the major elements of red mud leachate, Cl⁻ is derived from CaCl₂. CaCl₂ is used to precipitate soluble hydroxides, aluminates, and carbonate. By adding CaCl₂, soluble alkaline substances can be converted to calcite (CaCO₃), hydrocalumite (Ca₄Al₂(OH)₁₂·CO₃), and aluminohydrocalcite (CaAl₂(CO₃)₂(OH)₄·3H₂O). The insoluble tricalcium aluminate (Ca₃Al₂O₆) existing in red mud will participate in forming soluble Al(OH)₄⁻ ions [44–46]. This precipitation process aims to lower the pH and alkalinity of the leachate before discharge. The F⁻ is mainly leached from the fluoride in red mud, derived from the bauxite ore. The F⁻ content in red mud leachate is more than 44 times higher than the recommended value of USEPA (GW) and China (GW) (Figure 3, Table 6). The long-term intake of water with high fluoride concentration may cause bone fluorosis, dental fluorosis, osteoporosis, resulting in serious human health issues.

The concentrations of minor and trace elements, such as As, B, Cr, Fe, Ni, Mn, Mo, V, Zn, Ag, Be, Cd, Co, Hg, Pb, Sb, Se, and Tl, exceed the standards. The heavy metal elements, such as Cr, Fe, Ni, Mn, Mo, V, Zn, Ag, Co, Hg, and Pb, derived from the metal and its associated minerals in bauxite ore. These heavy metal elements could accumulate in soil and water. They increase ecological risks to crops, agricultural products, and groundwater, and also endanger human health through the food chain [47]. The impacts of red mud and its associated leachate on the surrounding environment largely depend on the management of red mud. Measures to prevent the leakage or spill of red mud and its leachate should be considered in the design of red mud management facilities, especially in the design of the containment system (especially, the liner) of the red mud reservoirs. Therefore, further studies are needed to investigate the compatibility between red mud leachate and liner materials, as the chemical environment, especially high pH and salinity conditions, could affect the hydraulic behavior and strength of the liner materials [48–50].

5. Conclusions

This study evaluated the chemical and mineralogical composition of red mud produced in China. Red mud and leachate samples were taken from five management facilities in Shandong, Guangxi, and Henan provinces of China. The chemical and mineralogical compositions of red mud and the major, minor and trace elements in the leachate were evaluated by laboratory analytical methods. The results of geochemical analysis on red mud from the literature were compared for a better understanding of the chemical characteristics of red mud.

Based on the findings of this study, the following conclusions and recommendations are drawn:

- The major chemical components of red mud are SiO₂, TiO₂, Al₂O₃, Fe₂O₃, CaO, and Na₂O, and the secondary components are K₂O, MgO, P₂O₅, MnO, Cr₂O₃, and SO₃. The main minerals include quartz, calcite, dolomite, hematite, hibschite, sodalite, anhydrite, cancrinite, and gibbsite.
- The mineral and chemical compositions of red mud vary over different alumina refining processes and parental bauxite. Diaspore is the primary type of bauxite in China. Among the red mud produced by the Bayer, sintering, and combined methods, levels of Na₂O and Al₂O₃ are higher in the red mud from the Bayer method, and CaO is higher in red muds from the sintering method.
- The major elements and ions in red mud leachates include Al, Ca, Cl⁻, F⁻, K, Na, Mg, NO₃²⁻, Si, and SO₄²⁻. The concentrations of Al, Cl⁻, F⁻, Na, NO₃²⁻, and SO₄²⁻ exceed the recommended groundwater quality standard of China by up to 6637 times. These ions are likely to increase the salinization in the soil and groundwater.
- The minor elements in red mud leachates include As, B, Ba, Cr, Cu, Fe, Ni, Mn, Mo, Ti, V, and Zn, while the trace elements in red mud leachate include Ag, Be, Cd, Co, Hg, Li, Pb, Sb, Se, Sr, and Tl. The concentrations of these elements are 2.4 to 272.0 times higher than the MCLs of China (GW) and USEPA (GW). These heavy metal elements could accumulate in soil and water, increase ecological risks to crops, agricultural products, and groundwater, and endanger human health through the food chain.

Author Contributions: Conceptualization, J.C. and X.L.; methodology, J.C.; validation, J.C., and K.T.; formal analysis, J.C. and C.S.; investigation, J.C. and K.T.; resources, X.W. and D.P.; data curation, C.S. and J.C.; writing—original draft preparation, C.S, J.C. and X.L.; writing—review and editing, K.T. and J.C.; visualization, C.S.; supervision, X.W. and D.P.; funding acquisition, J.C. and X.L.

Funding: This research was funded by the National Natural Science Foundation of China (No. 41701347 and 41502269). The field trip and APC is also Supported by the Foundation of Key Laboratory of Soft Soils and Geoenvironmental Engineering (Zhejiang University), Ministry of Education (no. 2019P04) and Sichuan Science and Technology Program (no. 2019YJ0244).

Acknowledgments: The authors would acknowledge the help and support from Dean Craig H. Benson (University of Virginia), Nuo-yi Yang (University of Wisconsin), and Donna Wang (from Jiegao Technology Inc., China).

Conflicts of Interest: The authors declare no conflict of interest.

References

1. Kishida, M.; Harato, T.; Tokoro, C.; Owada, S. In situ remediation of bauxite residue by sulfuric acid leaching and bipolar-membrane electrodialysis. *Hydrometallurgy* **2017**, *170*, 58–67. [CrossRef]
2. USGS. Bauxite and Alumina. 2016. Available online: <http://minerals.usgs.gov/minerals/pubs/commodity/bauxite/mcs-2016-bauxi.pdf> (accessed on 1 January 2016).
3. Han, Y.S.; Ji, S.; Lee, P.K.; Oh, C. Bauxite residue neutralization with simultaneous mineral carbonation using atmospheric CO₂. *J. Hazard. Mater.* **2017**, *326*, 87–93. [CrossRef]
4. Xue, S.; Kong, X.; Zhu, F.; Hartley, W.; Li, X.; Li, Y. Proposal for management and alkalinity transformation of bauxite residue in China. *Environ. Sci. Pollut. Res.* **2016**, *23*, 12822–12834. [CrossRef]
5. Liu, W.; Chen, X.; Li, W.; Yu, Y.; Yan, K. Environmental assessment, management and utilization of red mud in China. *J. Clean. Prod.* **2014**, *84*, 606–610. [CrossRef]
6. Burke, I.T.; Mayes, W.M.; Peacock, C.L.; Brown, A.P.; Jarvis, A.P.; Gruiz, K. Speciation of arsenic, chromium, and vanadium in red mud samples from the Ajka spill site, Hungary. *Environ. Sci. Technol.* **2012**, *46*, 3085–3092. [CrossRef] [PubMed]
7. Anton, A.; Rékási, M.; Uzinger, N.; Széplábi, G.; Makó, A. Modelling the potential effects of the hungarian red mud disaster on soil properties. *Water Air Soil Pollut.* **2012**, *223*, 5175–5188. [CrossRef]
8. Li, R.; Zhang, T.; Liu, Y.; Zhou, J.; Zou, R.; Kuang, S. Characteristics of red mud slurry flow in carbonation reactor. *Powder Technol.* **2017**, *311*, 66–76. [CrossRef]
9. Ruyters, S.; Mertens, J.; Vassilieva, E.; Dehandschutter, B.; Smolders, E. The Red Mud Accident in Ajka (Hungary): Plant Toxicity and Trace Metal Bioavailability in Red Mud Contaminated Soil. *Environ. Sci. Technol.* **2011**, *45*, 1616–1622. [CrossRef] [PubMed]

10. Lockwood, C.L.; Stewart, D.I.; Mortimer, R.J.G.; Mayes, W.M.; Jarvis, A.P.; Gruiz, K.; Burke, I.T. Leaching of copper and nickel in soil-water systems contaminated by bauxite residue (red mud) from Ajka, Hungary: The importance of soil organic matter. *Environ. Sci. Pollut. Res.* **2015**, *22*, 10800–10810. [[CrossRef](#)] [[PubMed](#)]
11. Rubinos, D.A.; Barral, M.T. Fractionation and mobility of metals in bauxite red mud. *Environ. Sci. Pollut. Res.* **2013**, *20*, 7787–7802. [[CrossRef](#)]
12. Habbashi, F. *Textbook of Hydrometallurgy; Métallurgie Extractive Québec*: Quebec City, Canada, 1999.
13. Bi, S. *Technics of Alumina Production*; Chemical Industry Press: Beijing, China, 2006. (In Chinese)
14. Liu, Z. Study on the mineral composition of Xinxu bauxite in Jingxi county. *Guangxi Southern Land Resour.* **2005**, *11*, 30–32. (In Chinese)
15. Yu, X. Mineral composition characteristics and beneficiability analysis of bauxite in Henan province. *Conserv. Util. Miner. Resour.* **2009**, *4*, 45–49. (In Chinese)
16. Ye, J.; Zhang, W.; Shi, D. Properties of an aged geopolymer synthesized from calcined ore-dressing tailing of bauxite and slag. *Cem. Concr. Res.* **2006**, *100*, 23–31. [[CrossRef](#)]
17. Yin, S. *The Research on Flue Gas Desulfurization of Red Mud Leaching Solution*; Beijing University of Chemical Technology: Beijing, China, 2014. (In Chinese)
18. Fu, G.; Tian, F.; Quan, K. Study on digestion of Chinese Middle/Low grade bauxite in Lime Bayer Process. *J. Northeast. Univ.* **2005**, *26*, 76–78. (In Chinese)
19. da Costa, M.L.; da Cruz, G.S.; de Almeida, H.D.F.; Poellmann, H. On the geology, mineralogy and geochemistry of the bauxite-bearing regolith in the lower Amazon basin: Evidence of genetic relationships. *J. Geochem. Explor.* **2014**, *146*, 58–74. [[CrossRef](#)]
20. Zarasvandi, A.; Carranza, E.J.M.; Ellahi, S.S. Geological, geochemical, and mineralogical characteristics of the Mandan and Deh-now bauxite deposits, Zagros Fold Belt, Iran. *Ore Geol. Rev.* **2012**, *48*, 125–138. [[CrossRef](#)]
21. Calagari, A.A.; Abedini, A. Geochemical investigations on Permo-Triassic bauxite horizon at Kanisheeteh, east of Bukan, West-Azarbaidjan, Iran. *J. Geochem. Explor.* **2007**, *94*, 1–18. [[CrossRef](#)]
22. Baioumy, H. Factors controlling the geochemical variations of lateritic bauxites formed upon different parent rocks in Peninsular Malaysia. *Arab. J. Geosci.* **2016**, *9*, 1–15. [[CrossRef](#)]
23. European Aluminum Association. *Bauxite Residue Management: Best Practice*; World Aluminum: Brussels, Belgium, 2013.
24. Zhang, Y.; Qu, Y.; Wu, S. Engineering geological properties and comprehensive utilization of the solid waste (red mud) in aluminium industry. *Environ. Geol.* **2002**, *41*, 249–256. [[CrossRef](#)]
25. Gao, Y. *Study on Two-Stage Acid Leaching Process of Alumina and Iron Oxide from Guangxi Pingguo Alumina Corporation Produced Red Mud*; Taiyuan University of Technology: Taiyuan, China, 2014. (In Chinese)
26. Rao, P. Analysis on basic characteristics of bayer's dry red mud and the operation feature of the yard. *J. Eng. Geol.* **2010**, *18*, 340–344. (In Chinese)
27. Liang, L. Contrastive analysis of phase and percentage of red mud in different places of Guangxi. *Technol. Dev. Chem. Ind.* **2012**, *41*, 39–40. (In Chinese)
28. Liu, Y.; Ni, W.; Huang, X.; Li, D.; Ma, X. Hydraulic cementitious properties of bayer process red mud from Guangxi Pingguo aluminium corporation. *Met. Mine* **2016**, *7*, 193–196. (In Chinese)
29. Jiang, Y.; Ning, P. An overview of comprehensive utilization of red mud from aluminum production. *Environ. Sci. Technol.* **2003**, *1*, 40–42. (In Chinese)
30. Liao, C.; Lu, H.; Qiu, D.; Xu, X. Recovering valuable metals from red mud generation during alumina production. *Light Met.* **2003**, *10*, 18–22. (In Chinese)
31. Liu, C. *The Feasibility Investigation to the Concrete Made by the Red Mud for Zhongzhou Aluminium Factory*; Henan Polytechnic University: Jiaozuo, China, 2007. (In Chinese)
32. Zhuo, J. *Study on Adsorption of Red Mud for Heavy Metal Cr⁶⁺ in Water*; Taiyuan University of Technology: Taiyuan, China, 2010. (In Chinese)
33. Wang, P. Characteristics and rapid hardening mechanism of red mud from alumina production with sintering process. *Nonferrous Met.* **2005**, *57*, 115–119. (In Chinese)
34. Li, Y.; Liu, C.; Luan, Z.; Peng, X.; Zhu, C.; Chen, Z.; Zhang, Z.; Fan, J.; Jia, Z. Phosphate removal from aqueous solutions using raw and activated red mud and fly ash. *J. Hazard. Mater.* **2006**, *137*, 374–383. [[CrossRef](#)]
35. Yu, Q.; Zhou, M.; Li, M. Comprehensive utilization of red mud and its application in environmental protection. *J. Jiangxi Chem. Ind.* **2007**, *4*, 126–127. (In Chinese)

36. Liu, S.; Xie, G.; Li, R.; Yu, Z. Comprehensive utilization of the red mud from alumina plant. *Min. Metall.* **2015**, *24*, 72–75. (In Chinese)
37. Wang, K.; Li, A.; Deng, H.; Zhu, G. Physicochemical properties of red mud in Shanxi. *Light Met.* **2012**, *4*, 25–28. (In Chinese)
38. Ellahi, S.S.; Taghipour, B.; Zarasvandi, A.; Bird, M.I.; Somarin, A.K. Mineralogy, Geochemistry and Stable Isotope Studies of the Dopolan Bauxite Deposit, Zagros Mountain, Iran. *Minerals* **2016**, *6*, 11. [[CrossRef](#)]
39. Chen, J.; Bradshaw, S.; Benson, C.H.; Tinjum, J.M.; Edil, T.B. ph-dependent leaching of trace elements from recycled concrete aggregate. In Proceedings of the American Society of Civil Engineers Geocongress, Oakland, CA, USA, 25–29 March 2012; pp. 3729–3738.
40. Power, G.; Gräfe, M.; Klauber, C. Bauxite residue issues: I. Current management, disposal and storage practices. *Hydrometallurgy* **2011**, *108*, 33–45. [[CrossRef](#)]
41. Borra, C.R.; Blanpain, B.; Pontikes, Y.; Binnemans, K.; Van Gerven, T. Recovery of Rare Earths and Major Metals from Bauxite Residue (Red Mud) by Alkali Roasting, Smelting, and Leaching. *J. Sustain. Metall.* **2017**, *3*, 393–404. [[CrossRef](#)]
42. Han, Y.; Yang, J.; Wang, X.; Li, J. Research on the basic characteristics and utilization value of the sintering process and Bayer process red mud. *Mater. Rep. B* **2011**, *22*, 122–125.
43. Gräfe, M.; Power, G.; Klauber, C. Bauxite residue issues: III. Alkalinity and associated chemistry. *Hydrometallurgy* **2011**, *108*, 60–79. [[CrossRef](#)]
44. Blenkinsop, R.D.; Currell, B.R.; Midgley, H.G.; Parsonage, J.R. The carbonation of high alumina cement, Part I. *Cem. Concr. Res.* **1985**, *15*, 276–284. [[CrossRef](#)]
45. Whittington, B.I.; Fallows, T.M.; Willing, M.J. Tricalcium aluminate hexahydrate (TCA) filter aid in the Bayer industry: Factors affecting TCA preparation and morphology. *Int. J. Miner. Process.* **1997**, *49*, 1–29. [[CrossRef](#)]
46. Palmer, S.J.; Frost, R.L.; Smith, M.K. Minimising reversion, using seawater and magnesium chloride, caused by the dissolution of tricalcium aluminate hexahydrate. *J. Colloids Interface Sci.* **2011**, *353*, 398–405. [[CrossRef](#)]
47. Sun, X.; Ning, P.; Tang, X.L.; Yi, H.; Zhou, L.; Li, K. Heavy metals pollution assessment in soil surrounding Red Mud Ponds in Shaanxian, Henan. *J. Northwest A&F Univ.* **2015**, *43*, 122–128.
48. Kazempour, M.; Sundstrom, E.A.; Alvarado, V. Effect of alkalinity on oil recovery during polymer floods in Sandstone. *SPE Reserv. Eval. Eng.* **2012**, *15*, 195–209. [[CrossRef](#)]
49. Athanassopoulos, C.; Benson, C.; Chen, J.; Donovan, M. Hydraulic Conductivity of a Polymer-Modified GCL Permeated with High-pH Solutions. In Proceedings of the Geosynthetics 2015, Portland, OR, USA, 15–19 February 2015; IFAI: St. Paul, MN, USA, 2015; pp. 181–186.
50. Chen, J.; Benson, C.H.; Edil, T.B. Hydraulic Conductivity of Geosynthetic Clay Liners with Sodium Bentonite to Coal Combustion Product Leachates. *J. Geotech. Geoenviron. Eng.* **2018**, *144*, 04018008. [[CrossRef](#)]



© 2019 by the authors. Licensee MDPI, Basel, Switzerland. This article is an open access article distributed under the terms and conditions of the Creative Commons Attribution (CC BY) license (<http://creativecommons.org/licenses/by/4.0/>).